Nonlinear Saturation and Determination of the Two-Photon Absorption Cross Section of Green Fluorescent Protein

Sean M. Kirkpatrick,[†] Rajesh R. Naik,[†,‡] and Morley O. Stone*,[†]

Materials and Manufacturing Directorate, Air Force Research Laboratory, Wright-Patterson Air Force Base, Ohio 45433-7702, and Technical Management Concepts Inc., Beavercreek, Ohio 44543

Two-photon absorption is a nonlinear phenomenon that is observed in materials irradiated with the combined energy of two photons, which matches the transition energy between the ground state and the excited state. Molecules exhibiting strong two-photon absorption have great potential in a wide range of applications such as three-dimensional fluorescence imaging, optical data storage, and microfabrication.[9,6] Green fluorescent protein (GFP) can be excited by a two-photon mechanism and exhibits a nonlinear behavior of the effective two-photon absorption coefficient. Here we present the quantitative determination of the two-photon absorption saturation of GFP in both a homogeneously broadened and inhomogeneously broadened system. We further show that, dominated by strong nonlinear saturation, GFP has a large intrinsic two-photon absorption cross section (σ_{TPA}) value that is several orders of magnitude larger than that of chemically synthesized compounds.

Introduction

Green fluorescent protein (GFP) from *Aequorea victoria* has become an important tool in cell biology and has been extensively used in monitoring gene expression and intracellular protein localization.[10] The chromophore of GFP is formed by the autocatalytic, posttranslational cyclization, and oxidation of the tripeptide Ser[65]–Tyr[66]–Gly[67] in the primary structure of the expressed protein.[7] Wild-type GFP has two absorption maxima: 396 and 476 nm. The absorption peaks correspond to the neutral and anionic chromophore states, respectively, that relax to a common emission state to generate the greenish-yellow fluorescence at 509 nm.[2] The background protein host shows a typical absorption edge at approximately 300 nm due to the aromatic substituents.

Molecular excitation via the simultaneous absorption of two photons has been shown to be of promise in the development of three-dimensional microfabrication, fluorescence imaging, and optical storage. The two-photon absorption process depends quadratically on the incident radiation intensity; therefore, the absorption and subsequent fluorescence is highly localized within the focal plane. GFP has been demonstrated to be a good flurophore for two-photon excitation, readily excited by 800 nm laser pulses, and has a two-photon excitation spectrum similar to that of the corresponding linear spectra.[19,17] While numerous articles have used GFP in a two-photon manner, the quantitation of this two-photon cross section is missing from the literature.[11,19,17] The cross section reported by Xu et al. (1996) on WT-GFP was termed the action cross section defined by the nonlinear quantum efficiency times the two-photon absorption cross section. This was due to a lack of independent measurement of the nonlinear quantum efficiency. However, if it is assumed that the linear and nonlinear quantum efficiencies are identical, then that work suggests a cross section of 3 Goppert–Meyers (GM) at around 790 nm. Note that this number is quoted by Volkmer et al. (2000) in performing their calculations. Schwille et al. estimates a posteriori the TPA cross section of EGFP to be 180 GM at 920 nm.[12] We feel that this variation among mutants and the subsequent understanding of the saturation behavior is important for the comparison of biological chromophores with synthetic chromophores and may lead to the discovery of novel photochemical applications.

In this work, the two-photon absorption cross section of GFP is investigated using standard ultrafast Z-scan measurements, nonlinear fluorescence measurements, semiclassical modeling, and beam propagation modeling. It is found that the TPA coefficient behaves nonlinearly with peak intensity, consistent with the saturation of the nonlinear fluorescence emission reported by Volkmer et al. (2000). In that work, several different mechanisms were cited as possible explanations for the observed saturation; however, it was speculated that the singlet-state absorption was responsible and that only a rate equation formalism would be able to quantify the dynamics. In that work, it is entirely feasible that excited-state absorption could be removing populations from the two-photon state due to the high repetition rate of the experiment (250 kHz). However, while explanations of the nonlinear behavior have been linked to the excited-state absorption, we demonstrate that the effect at low repetition rate (<500 Hz) and short pulse width (90 fs) is due to saturable two-photon absorption of the GFP chromophore and that the excited-state absorption is due primarily to the protein background. The functional form of the effective two-photon absorption coefficient depends on whether the absorption is homogeneously broadened or inhomogeneously broadened within the time frame of the experiment. A comparison of the respective theoretical forms of the effective TPA coefficient to the data is presented and discussed with respect to the systems dynamics. Quantitative TPA cross sections above and below saturation as well as an excited-state cross section are reported, and comparison to a formal rate equation analysis is given.

[†] Wright-Patterson Air Force Base.
[‡] Technical Management Concepts Inc.

Theoretical Background

Linear saturated absorption is well understood and often treated in nonlinear optics courses.[1] The theoretical treatment of a homogeneously broadened two-level-system, under steady-state conditions, leads to an intensity-dependent linear absorption coefficient (α^H) given by

$$\alpha^H = \frac{\alpha_0}{1 + I/I_{\text{sat,H}}} \tag{1}$$

where the homogeneous saturation intensity is given by

$$I_{\text{sat,H}} = \frac{\hbar\omega}{\tau\sigma_0\left(1 + \dfrac{g_k}{g_n}\right)} \tag{2}$$

Here, g_k (g_n) is the electronic degeneracy of the upper (lower) state, τ is the lifetime of the upper state, ω is the excitation frequency, and α_0 (σ_0) is the linear absorption (cross section) coefficient. Boyd (1992) has shown that in the case of linear saturated absorption, many saturable absorbing systems are imperfect[1] and do not obey the typical intensity dependent absorption coefficient given by eqs 1 and 2 but instead obey

$$\alpha^H = \frac{\alpha_0}{1 + I/I_{\text{sat,H}}} + \alpha_1 \tag{3}$$

where α_1 is a constant denoting the above saturation linear absorption coefficient linked to the background absorption of the host material (Boyd R. W., personal communication). The constant background absorption coefficient does not show saturation due to the high concentration of the host material relative to the photon density.

Here, we consider an analogous derivation of the two-photon saturation coefficient and its application to ultrafast measurements of the TPA behavior of GFP. Similar saturation effects have been modeled via a density matrix approach with respect to optical phase conjugation,[4] a semiperturbative approach with respect to molecular quantum wires,[16] and a hyperbolic approximation based on eq 1 for bulk semiconductors.[8] This work examines the question of whether a system of GFP chromophores in solution is homogeneously or inhomogeneously broadened under ultrafast experimental conditions. Both forms of the saturated two-photon absorption coefficient (homogeneous and inhomogeneous) are derived by extending the linear rate equation analysis for the two-level system to the nonlinear regime. The effects of excited-state absorption are then included, and a comparison of our model to the TPA behavior of GFP is presented.

Homogeneously Broadened Saturated Two-Photon Absorption Coefficient. From quantum mechanics, the transition rate of a two-photon absorption event from a state $|n\rangle$ to a state $|k\rangle$ is

$$W_{nk} = \left[\frac{\mu_{nm}\mu_{mk}}{\omega_{mn} - \omega}\right]^2 \frac{2\pi|E|^4 g(\omega_{kn})}{8\hbar^4} \tag{4}$$

where the Einstein summation notation is implied for the virtual states $|m\rangle$ within the square brackets, and a normalized homogeneously broadened line shape, $g(\omega_{kn})$, is assumed. Using the definition of intensity as $I = [(\epsilon c)/(2n_0)]|E|^2$ with n_0 being the linear index of refraction, we can rewrite the two-photon absorption transition rate as

$$W_{nk} = \frac{\sigma_{\text{TPA}}I^2}{2\hbar\omega} \tag{5}$$

where the two-photon absorption cross section is given in units of cm⁴/GW and embodies the dipole moments, line shape, and constant factors in eq 4. If both linear absorption and excited-state absorption are ignored, then the rate equations governing this two-level system are

$$\frac{dN_k}{dt} = -W_{nk}\left(N_k - \frac{g_k}{g_n}N_n\right) - \frac{N_k}{\tau_{kn}}$$

$$\frac{dN_n}{dt} = -\frac{dN_k}{dt} \tag{6}$$

where τ_{kn} is the lifetime of the upper state and g_k(g_n) is the electronic degeneracy of the upper (lower) state. Using the localized coordinate transformations $\zeta = z$ and $\eta = z - ct$, we then take the propagation equation to be (again, assuming negligible linear absorption)

$$\frac{dI}{d\zeta} = 2\hbar\omega W_{nk}\left(N_k - \frac{g_k}{g_n}N_n\right) = \sigma_{\text{TPA}}\Delta N I^2 \tag{7}$$

where $\Delta N = N_k - [(g_k)/(g_n)]N_n$. If it is assumed that we have at least a quasi-steady-state regime, then using the localized coordinate transformations, eq 6 can be rewritten as

$$\frac{d\Delta N}{d\eta} = 0 = -\left(1 + \frac{g_k}{g_n}\right)W_{nk}\Delta N - \left(\frac{\dfrac{g_k}{g_n}N_0 + \Delta N}{\tau_{kn}}\right) \tag{8}$$

where $N_0 = N_k + N_n$ is the total concentration of the two-photon absorbers. Extending the derivation given by Yariv (1989) for the linear saturated absorption model, we can solve for the equilibrium population inversion ΔN^{eq} from eq 8 and substitute it into eq 7. It follows that for a homogeneously broadened system, the propagation equation dominated by two-photon absorption is given by

$$\frac{dI}{d\zeta} = \frac{-\sigma_{\text{TPA}}I^2\dfrac{g_k}{g_n}N_0}{[1 + I^2/I_{\text{sat,H}}^2]} \tag{9}$$

where we have identified the square of the homogeneous saturation intensity as

$$I_{\text{sat,H}}^2 = \frac{2\hbar\omega}{\tau_{kn}\sigma_{\text{TPA}}\left(1 + \dfrac{g_k}{g_n}\right)} \tag{10}$$

The homogeneously broadened effective two-photon absorption coefficient can then be identified from eq 9 as

$$\beta_{\text{eff}}^H(I) = \frac{\sigma_{\text{TPA}}\dfrac{g_k}{g_n}N_0}{[1 + I^2/I_{\text{sat,H}}^2]} \tag{11}$$

Note that at low intensities, this reduces to the normal definition of the two-photon absorption coefficient in terms of the cross section.

Absorption of Green Fluorescent Protein

J. Phys. Chem. B, Vol. 105, No. 14, 2001 **2869**

Inhomogeneously Broadened Saturated Two-Photon Absorption Coefficient. If we continue to follow the analogous derivation of the linear saturated absorption coefficient, it is straightforward to show that the inhomogeneously broadened system will have a saturated two-photon absorption coefficient given by

$$\beta_{\text{eff}}^{\text{Inh}}(I) = \int_{-\infty}^{\infty} \beta_{\text{eff}}^{\text{H}}(I, \omega - \omega_{kn}) p(\omega_{kn}) \, d\omega_{kn} \quad (12)$$

where $p(\omega_{kn})$ is the probability of a homogeneous class of absorbers having a central frequency of ω_{kn} and $\omega - \omega_{kn}$ has explicitly been included in the argument of the homogeneous TPA coefficient to point out the dependence buried in the homogeneous line shape, $g(\omega_{kn})$, of the TPA cross section. Under the approximation that the inhomogeneous line shape is slowly varying with respect to the homogeneous line shape (assumed to be a Lorentzian), evaluation of eq 12 results in

$$\beta_{\text{eff}}^{\text{Inh}}(I) = \frac{\sigma_{\text{TPA}}^{\text{Inh}} \frac{g_k}{g_n} N_0}{\sqrt{1 + I^2/I_{\text{sat,Inh}}^2}} \quad (13)$$

where $\sigma_{\text{TPA}}^{\text{Inh}}$ and the inhomogeneous saturation intensity are defined by

$$\sigma_{\text{TPA}}^{\text{Inh}} = p(2\omega) \left[\frac{\mu_{nm}\mu_{mk}}{\omega_{mn} - \omega} \right]^2 \frac{2\pi^2 n_0^2 \omega}{\hbar^3 \epsilon^2 c^2} \quad (14)$$

$$I_{\text{sat,Inh}}^2 = \frac{\hbar\omega\Delta\omega\pi p(2\omega)}{\tau_{kn}\left(1 + \frac{g_k}{g_n}\right)\sigma_{\text{TPA}}^{\text{Inh}}}$$

Here, $p(2\omega)$ is the probability of a homogeneous class of absorbers having a central frequency of 2ω. Analogously, this is the normalized inhomogeneous line shape function. The quantity $\Delta\omega$ is related to the dephasing time of the excitation, i.e., the width of the homogeneous line shape, $g(\omega_{kn})$. The semiclassical expressions derived in eqs 11–14 are similar to those found from a purely quantum mechanical approach as previously described.[4] We again note that if the intensity is very low compared to the saturation intensity, then eq 13 reduces to the typical expression.

Excited-State Absorption and Background Contributions. Until now, we have been examining the saturation behavior of the chromophore nonlinearity. Noting that the observed saturation does not go to zero, it is assumed that a second contribution, that of the protein background, is contributing to the nonlinear absorption similar to the linear case of eq 3. Apart from an additional constant TPA coefficient, the effective nonlinear coefficient has a finite positive slope above the saturation intensity, indicating the possibility of excited-state absorption. To fully model the system, we consider the general case of excited-state absorption from a two-photon absorption event. For a three level system, in the absence of stimulated emission (and subsequently from saturation), it can be shown that under short pulse excitation, the two-photon excited-state population can be approximated as

$$N_k \approx \frac{\sigma_{\text{TPA}}\frac{g_k}{g_n}N_0\tau_{\text{p}}I_0^2}{2\hbar\omega}\sqrt{\frac{\pi}{2}} \quad (15)$$

where τ_{p} is the pulse width and I_0 is the peak intensity from a

Gaussian pulse.[15] Assuming the excited-state absorption depends only on the two-photon excited-state population, N_k, the propagation equation becomes (linear absorption negligible)

$$\frac{\text{d}I}{\text{d}\zeta} = -\sigma_{\text{TPA}}\frac{g_k}{g_n}N_0I^2 - \sigma_{\text{ESA}}N_kI \quad (16)$$

Substituting eq 15 into eq 16, factoring out an I^2, and performing a Taylor expansion on the Gaussian pulse profile, one can identify (to lowest order) the effective two-photon absorption coefficient as

$$\beta_{\text{eff}}^{\text{H}}(I \ll I_{\text{sat,H}}) = \beta_0^{\text{H}}\left(1 + \frac{\sigma_{\text{ESA}}\tau_{\text{p}}I_0}{2\hbar\omega}\sqrt{\frac{\pi}{2}}\right) \quad (17)$$

where $\beta_0^{\text{H}} = \sigma_{\text{TPA}}(g_k/g_n)N_0$. The linear dependence of the two-photon absorption coefficient on intensity is manifested in typical Z-scan or nonlinear transmission experiments where the excitation energy is varied and the effective TPA coefficient measured as a function of intensity. The resulting data are fitted to a line giving the *y*-intercept as the TPA coefficient and the slope as being proportional to the excited-state absorption. It can again be shown that the analogous inhomogeneous expression of eq 17 can be found from evaluation of eq 12, resulting in

$$\beta_{\text{eff}}^{\text{Inh}}(I) = \sigma_{\text{TPA}}^{\text{Inh}}\frac{g_k}{g_n}N_0\left(1 + \frac{\sigma_{\text{ESA}}\tau_{\text{p}}I_0}{2\hbar\omega}\sqrt{\frac{\pi}{2}}\right) \quad (18)$$

where we have assumed that the excited-state absorption cross section is nearly constant, such as occurs for excitation into or near the continuum or conduction bands.

Effective Two-Photon Absorption Coefficient. Taking into account the background absorption of a host material, it has already been noted that linear saturable absorbers behave according to eq 3. It is reasonable to expect that saturation of a two-photon absorber in a host background (protein background in this case) would behave similarly. Thus, we propose that for a system of absorbers having a low concentration compared to the photon density, the former saturation model (eq 11 or 13) would dominate. As the intensity is increased beyond the saturation intensity, any intrinsic TPA and ESA of the protein background become observable, allowing the later model (eq 17 or 18) to dominate. Under these conditions, it is expected that a measurement of the effective two-photon absorption coefficient using standard Z-scan routines will yield a plot fitting eq 11 or 13 at low intensities (but comparable to the saturation intensity) and fitting eq 17 or 18 at higher intensities. Subsequently, the cross section (or TPA coefficient) appearing in eq 17 and 18 is expected to be related to the protein background and is not expected to be the same as in eq 11 and 13, such that for $\sigma_{\text{ESA}} = 0$; an expression similar to eq 3 is obtained. The choice of the final form of the effective TPA coefficient will depend on whether the system is homogeneously or inhomogeneously broadened within the time frame of the experiment, in this case 90 fs. For the case of a homogeneously broadened system, a measurement of the TPA coefficient versus intensity should follow the form of

$$\beta_{\text{eff}}^{\text{H}}(I) = \frac{\beta_0^{\text{H}}}{[1 + I^2/I_{\text{sat,H}}^2]} + \beta_0^{\text{H,host}}\left(1 + \frac{\sigma_{\text{ESA}}\tau_{\text{p}}I_0}{2\hbar\omega}\sqrt{\frac{\pi}{2}}\right) \quad (19)$$

The analogous inhomogeneously broadened system will have the form

$$\beta_{\text{eff}}^{\text{Inh}}(I) = \frac{\beta_0^{\text{Inh}}}{\sqrt{1 + I^2/I_{\text{sat,Inh}}^2}} + \beta_0^{\text{Inh,host}}\left(1 + \frac{\sigma_{\text{ESA}}\tau_p I_0}{2\hbar\omega}\sqrt{\frac{\pi}{2}}\right) \quad (20)$$

Here, we have designated the above saturation TPA coefficients with a (host) in the superscript analogous to eq 3 for distinction. Note the difference in the functional form of the saturated terms of the models. The excited-state absorption cross section can be linked to either the protein host or chromophore species, depending on the coupling between the two-photon states of the protein and chromophore.

Beam Propagation Modeling Code. An additional method of modeling was employed to verify the saturation and excited-state absorption hypothesis. This method used a beam propagation model in conjunction with a set of rate equations describing the GFP system under ultrashort pulse excitation in order to simulate a Z-scan experiment. The basic premise of BPM analysis is described elsewhere in the literature.[18] The pulse profile is propagated through slices of the sample cell while simultaneously solving the following rate equations via a fourth order Runge−Kutta algorithm:

$$\frac{dN_p}{dt} = \frac{\sigma_{\text{ESA}}I}{\hbar\omega}N_k - \frac{N_p}{\tau_{pk}} - \frac{N_p}{\tau_{pn}}$$

$$\frac{dN_k}{dt} = -\frac{\sigma_{\text{TPA}}I^2}{2\hbar\omega}\left(N_k - \frac{g_k}{g_n}N_n\right) - \frac{\sigma_{\text{ESA}}I}{\hbar\omega}N_k + \frac{N_p}{\tau_{pk}} - \frac{N_k}{\tau_{k2}}$$

$$\frac{dN_{k2}}{dt} = \frac{N_k}{\tau_{k2}} - \frac{N_{k2}}{\tau_{kn}} \quad (21)$$

$$\frac{dN_n}{dt} = -\frac{N_n}{\tau_{n2}} + \frac{N_{k2}}{\tau_{kn}}$$

$$\frac{dN_{n2}}{dt} = -\frac{dN_k}{dt} - \frac{dN_p}{dt} - \frac{dN_n}{dt} - \frac{dN_{k2}}{dt}$$

where n, k, and p denote the ground-state manifold, first excited-state manifold (reached through a TPA event), and a higher-lying excited state (reached via a one photon absorption event from k), respectively. A manifold letter accompanied by a subscript 2 indicates the lowest level of that manifold. Two letters in the subscript of τ designates a radiative lifetime between manifolds, and dephasing or nonradiative lifetimes within the manifold are designated by the subscript 2. Note that this model is necessarily a homogeneous model. Fluorescence lifetimes and dephasing rates were taken from the literature[2,17] and are on the nanosecond and picosecond time scales, respectively. The resulting transmission simulating the open aperture Z-scan is then fit using standard fitting routines. The effective two-photon absorption coefficient is plotted versus peak intensity and is shown in Figure 1. The solid line is a fit using eq 19 above. While qualitative agreement with our model is demonstrated, quantitative BPM agreement with the data cannot be obtained due to the nature of an inhomogeneous model and the intractable problem of solving an infinite number of rate equations. The main purpose of this analysis is to demonstrate that under high peak intensity, short pulse excitation, a low concentration of TPA absorbers can reach a steady state, showing saturation. Consequently, the use of a two-level model to describe TPA saturation by a steady-state mechanism under ultrashort pulse excitation is justified. Also, note that loss due to a host species is not taken into account in eq 21 and that the two-photon absorption coefficient above and below saturation becomes the same, as is found from the fit to the simulation.
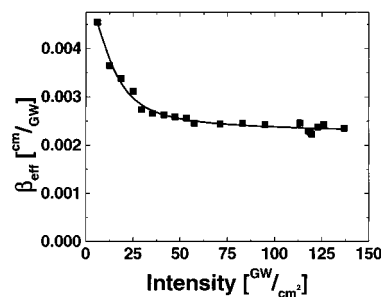

Figure 1. Beam propagation modeling (BPM) simulation illustrating the two-photon saturation effect of a homogeneously broadened two level system under high intensity ultrashort pulsed excitation. The solid line is the theoretical fit using the homogeneously broadened model.

Experimental Section

Expression and Purification of GFP. A polyhistidine-tagged GFP was expressed in *Escherichia coli* using the expression plasmid pET22b (Novagen), wherein the coding region of GFPuv (cycle 3 mutant) was fused in-frame with a carboxyl-terminal polyhistidine tag. The recombinant GFP was expressed in bacterial strain BL21 (DE3) after induction with IPTG (1mM) at 30 °C and purified by nickel affinity chromatography. Protein purity was confirmed by SDS-PAGE. The purified sample was dialyzed against 10 mM sodium phosphate buffer pH 7.0 and stored at −20 °C. All spectroscopic measurements were done with 5−20 μM of GFP in 25% dimethyl sulfoxide (DMSO). The linear absorbance at 396 nm was used in calculating the concentration of the sample using Beer's law.

Z-scan Analysis. A standard Z-scan experiment was performed to measure the two-photon absorption cross section of GFP. GFP samples were prepared in 25% dimethyl sulfoxide in 1 cm spectroscopic cells, compared to the 10 cm Rayleigh range used in the experiment. A Ti:Sapphire femtosecond laser system with regenerative amplification system was used to generate bandwidth-limited 90 fs pulses, with pulse energies between 0.5 and 7 μJ centered at 800 nm at a repetition rate of 500 Hz. An additional set of experiments using a variable repetition rate was performed to remove concern over cumulative effects. The standard transmission functions for thin sample open aperture measurements were used to extract the effective two-photon absorption coefficient.[13]

Linear Fluorescence Spectroscopy. Fluorescence measurements of cell lysates prepared from equivalent number of cells, as measured by OD_{600}, were carried out on a Perkin-Elmer LS50B spectrofluorometer using 1 cm quartz cuvette. The excitation and emission wavelengths were set to 395 and 509 nm, respectively, with a slit width set between 5 and 12 nm.

Nonlinear Fluorescence Spectroscopy. Nonlinear fluorescence measurements of the same samples as those described above were carried out using a 1 cm quartz cuvette and a fiber coupled ISA Spex 270M spectrometer. The excitation wavelength was 800 nm with a 90 fs pulse at a repetition rate of less than 500 Hz. Pulse energy attenuation was accomplished using ultrafast polarizers and a thin variable ND filter with low dispersion. The entire emission band was collected on a liquid nitrogen CCD array and integrated to give the intensity dependence.

Results and Discussion

The excitation of GFP at 800 nm yielded the fluorescence spectra shown Figure 2. The overlay of linear and nonlinear fluorescence spectra resulting from excitation at 395 and 800 nm, respectively, demonstrates a close coupling of the one-
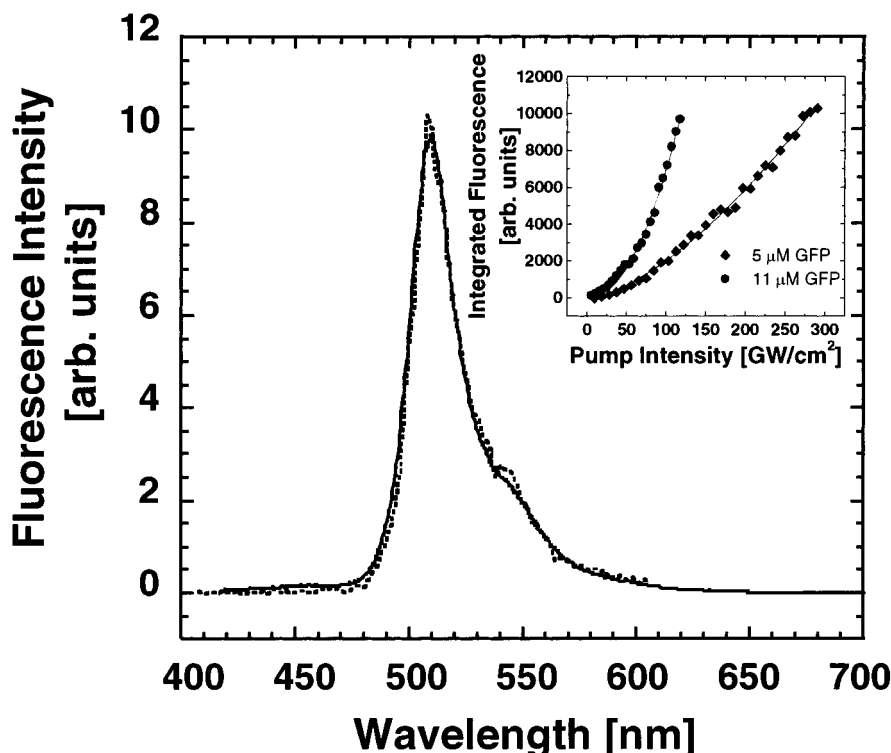
Absorption of Green Fluorescent Protein

J. Phys. Chem. B, Vol. 105, No. 14, 2001 **2871**

Figure 2. Linear (solid line) and nonlinear (dashed line) fluorescence of GFP resulting from excitation at 395 and 800 nm, respectively. The inset shows the integrated nonlinear fluorescence as a function of intensity for high and low concentrations of GFP. A deviation from the square power law is observed in the low concentration sample and is attributed to two-photon saturation.

photon and two-photon states after excitation. The inset to Figure 2 shows the integrated nonlinear fluorescence as a function of intensity for a high concentration (11 μM) sample and a sample at approximately half concentration (5 μM). The power law fit to the data at 11 μM gives an exponent of 2.0, indicating a dominant two-photon process. The fit to the data at half concentration gives an exponent of 1.5—clearly showing saturation.

The effective TPA coefficient (solid circles) of GFP as a function of peak intensity was measured by a standard open aperture Z-scan technique (Figure 3). The data were obtained from multiple identical samples over a period of several weeks. Some data points overlap. The data were fit using both the homogeneous and inhomogeneous models. It was found that the homogeneous model failed to approximate the data (not shown) while the inhomogeneous model fits well. The two dashed lines are the fits to the low intensity data using eq 13 and the high-intensity data using eq 18. The solid line is a fit using eq 20. The resulting fit parameters are identical to within error. The results are summarized in Table 1.

The corresponding two-photon absorption cross sections of the GFP chromophore and the protein background are found to be $\sigma_{\text{TPA}}^{\text{Inh}} = 2.4 \pm 0.8 \times 10^{-17}$ cm⁴/GW and $\sigma_{\text{TPA}}^{\text{host}} = 5.3 \pm 2.4 \times 10^{-19}$ cm⁴/GW, respectively. As the GFP chromophore cannot be removed from its β-barrel environment, a crude protein extract prepared from cells expressing a control plasmid was measured as an indication of the host contribution. The solid squares are the identical measurements of the crude protein extract. Note that the data lies on top of the theoretical fit to the high intensity data of GFP given by eq 18. The slopes are identical to within the experimental error, suggesting that the excited-state absorption is primarily due to the host protein. The ESA cross section of the protein background is found to be $1.25 \pm 0.6 \times 10^{-16}$ cm². The easily saturated chromophore leads to a nonlinear effect at longer pulse widths and higher energies,
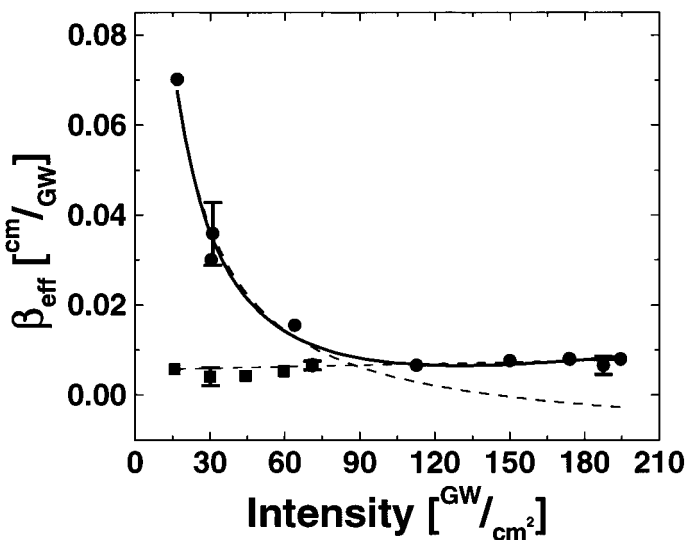

Figure 3. Effective TPA coefficient of (●) GFP and a control protein extract (■) as a function of peak intensity, as measured by a standard open-aperture Z-scan technique. The two dashed lines are the fits to the low-intensity data using eq 13 and the high-intensity data using eq 18. The solid line is a fit using eq 20.

TABLE 1: Fit Parameters of Inhomogeneously Broadened Saturated Two-Photon Absorption Coefficient with Excited-State Absorption (eqs 13, 18, and 20)

β_0^{Inh} (cm/GW)	$I_{\text{sat,Inh}}$ (GW/cm²)	$\beta_0^{\text{Inh,host}}$ (cm/GW)	σ_{ESA} (cm²)
0.16 ± 0.05	9.7 ± 3.1	0.0035 ± 0.0016	$1.25 \pm 0.6 \times 10^{-16}$

dominated by the protein background. As GFP cannot be made at large concentrations (mM) due to protein precipitation, accessing the high intrinsic TPA cross section of the chromophore is unlikely unless solid concentration densities are obtained. However, as nonlinear fluorescence is visible at higher

energies and longer pulse widths (i.e. above saturation), it is reasonable to surmise that the GFP chromophore quickly reaches an equilibrium, emitting fluorescence in steady state, while the protein background continues to absorb nonlinearly, although at a much reduced cross section. This hypothesis is consistent with the observation of Volkmer et al., (2000) where a saturation effect of the nonlinear fluorescence of GFP was observed. It should be noted, however, a higher concentration of GFP was used in that work (18 μM) versus the concentration used for our saturation measurements (5 μM), and subsequently, saturation occurred at a higher intensity (approximately 400 GW/cm^2 compared to 10 GW/cm^2).[17] It is interesting to note that Schwille et al. report a saturation intensity of about 0.01 GW/cm^2 when using a few hundred nanomolar concentration of EGFP. A plot of these three saturation intensities versus concentration shows a cubic concentration dependence (data not shown). It is conjectured that if saturation is occurring by the above mechanism, then the increase in concentration could be analogous to pressure broadening of gaseous systems (typically quadratic in a homogeneously broadened system). Alternatively, concentration quenching of the excited-state, which is known to occur at high (tens of micromolar) concentration, could also be responsible for the observed dependence. Further work on this detail would be needed to investigate the apparent cubic dependence.

It might be suggested that as both the protein background and GFP chromophore exhibit two-photon absorption at the same frequency and duration of order of the lifetime, energy transfer between the states may be possible and therefore may reduce the saturation effect by removing excited-state population from the chromophore. As the protein background shows absorption well into the 400 nm range, two-photon absorption of the contaminating protein molecules could result in energy transfer to the GFP chromophore via collisions or electron−phonon coupling within the lifetime of the excitation. It has been found, however, that linear excitation within the absorption band around 300 nm resulted in no fluorescence from the GFP chromophore, indicating no intramolecular decay and subsequent energy transfer between the species. In addition, within the time frame of this experiment (90 fs), the system is essentially frozen with respect to collisions and phonon dynamics. Therefore, if such a process occurred, it would not be observed here. Longer pulse excitations also failed to show a reduction in the saturation effect, giving essentially the same null result on the transmission as that of the crude extract of much lower cross section. A steady-state fluorescence level was observed in cases above saturation. These observations were simulated using the beam propagation model above, scaling for the homogeneous solution. Simulations were run at pulse widths ranging up to milliseconds and energies up to 10 J, with no noticeable nonlinear effect on the transmission of the beam. It should be noted that as both the linear fluorescence and absorption spectra of the GFP samples before and after Z-scan measurements were reproducible within error (data not shown), it can be concluded that the structure of the chromophore did not change upon exposure to the intense laser beam.

If we compare the background TPA cross section, i.e., the saturated cross section ($\sim$1100 GM), to the reported values of WT-GFP (action TPA cross section $\sim$3 GM) and EGFP (TPA cross section $\sim$180 GM) by Xu et al. (1996) and Schwille et al. (1999), it is suggestive that these other measurements are within the saturation region. This conjecture is supported by the fact that high repetition rates (80 MHz) are used by the above authors. With saturation evident and steady-state reached

TABLE 2: A Comparison of Two-Photon Cross Section Values

	σ (cm^4/GW)	G−M (10^{-50} cm^{4}s/photon)
GFP	2.4×10^{-17}	$\sim$600 000
AF-380[5]	8.0×10^{-21}	198
Cumpston et al.[3]	ND	1250
Spangler et al.[14]	ND	66 000

at such a high repetition rate, a convoluted cross section between the chromophore and the protein background is to be expected. While the saturated TPA cross section of GFP is slightly larger than most chromophores, the unsaturated TPA cross section is several orders of magnitude higher than any chemically synthesized dyes we have found. Cumpston et al. (1999) designed a class of π-conjugated compounds that exhibited large σ_{TPA} values.[3] Interestingly, the value of GFP is at least an order of magnitude higher than the best chemically synthesized compound (Table 2) measured on the same time scales. We believe that the large two-photon cross section of GFP is more than a function of the central chromophore and that the larger protein structure is contributing to the two-photon absorption process, since a truncated version of GFP failed to be excited by a two-photon mechanism (data not shown).

Conclusions

GFP offers many advantages over chemically synthesized molecules. The relative ease in producing large quantities of recombinant GFP by heterologous expression, the photostability of GFP, the fluorescent readout, and its large apparent two-photon absorption property make it an attractive candidate in applications such as data storage, diagnostics and other photochemistry applications. A measurement of the effective two-photon absorption coefficient shows that the system is apparently inhomogeneously broadened and that within the time scale of the experiment, 90 fs, the dynamics of the system are frozen. If one takes saturation into account, then the intrinsic two-photon cross section of the chromophore is found to be 600 000 GM, while the background protein has a cross section of $\sim$1100 GM. The lower cross sections reported elsewhere are most likely due to a combination of the two-photon saturation, and excited-state absorption from either high repetition rates or CW experiments.

References and Notes

(1) Boyd, R. W. *Nonlinear Optics*, 3rd ed.; Academic Press: New York, 1992.

(2) Chattoraj, M.; King, B. A.; Bublitz, G. U.; Boxer, S. G. *Proc. Natl. Acad. Sci. U.S.A.* **1996**, *93*, 8362−8367.

(3) Cumpston, B. H.; Ananthavel, S. P.; Barlow, S.; Dyer, D. L.; Ehrlich, J. E.; Erskine, L. L.; Heikal, A. A.; Kuebler, S. M.; Lee, S. I.-Y.; McCord-Maughon, D.; Qin, J.; Rockel, H.; Rumi, M.; Wu, X.-L.; Marder, S. R.; Perry, J. W. *Nature* **1999**, *398*, 51−54.

(4) Kauranen, M.; Gauthier, D. J.; Malcuit, M. S.; Boyd, R. W. *Phys. Rev. A* **1989**, *40*, 1908−1917.

(5) Kirkpatrick, S. M.; Denny, L. R.; Stone, M. O. *Proc. SPIE* **2000**, *3951*, 102−107.

(6) Kirkpatrick, S. M.; Baur, J. W.; Clark, C. M.; Denny, L. R.; Reinhardt, B. R.; Kannan, R.; Stone, M. O. *Appl. Phys. A* **1999**, *69*, 1−4.

(7) Kojima, S.; Hirano, T.; Niwa, H.; Ohashi, M.; Inouye, S.; Tsuji, F. *Tetrahedron Lett.* **1997**, *38*, 2875−2878.

(8) Lami, J.-F.; Gilliot, P.; Hirlimann, C. *Phys. Rev. Lett.* **1996**, *77*, 1637−1653.

(9) Maruo, S.; Kawata, S. *J. Microelectromechan. Sys.* **1998**, *7*, 411−415.

Absorption of Green Fluorescent Protein

J. Phys. Chem. B, Vol. 105, No. 14, 2001 **2873**

(10) Misteli, T.; Spector, D. L. *Nat. Biotechnol.* **1997**, *15*, 961−4.

(11) Potter, S. M.; Wang, C.-M.; Garrity, P. A.; Fraser, S. E. *Gene* **1996**, *173*, 25−31.

(12) Schwille, Petra; Haupts, Ulrich; Maiti, Sudipta; Webb, Watt W. *Biophys. J.* **1999**, *77*, 2251−2265.

(13) Sheik-Bahae, M.; Said, A. A.; Wei, T.-H.; Hagan, D. J.; Van Strylan, E. W. *J. Quant. Electron.* **1990**, *26*, 760.

(14) Spangler, C. W.; Elandaloussi, E. H.; Casstevens, M. K.; Kumar, D. N.; Weibel, J. F.; Burzynski, R. *Proc. SPIE* **1999**, *3798*, 117−122.

(15) Sutherland, R. L. *Handbook of Nonlinear Optics*; Marcel Dekker: New York, 1996.

(16) Torruellas, W. E.; Lawrence, B. L.; Stegeman, G. I.; Baker, G. *Optics Lett.* **1996**, *21*, 1777−1779.

(17) Volkmer, A.; Subramaniam, V.; Birch, D. J. S.; Jovin, T. M. *Biophys. J.* **2000**, *78*, 1589−1598.

(18) Weitzman, P. S.; Osterberg, U.; Dominic, V. *IEEE J. Quant. Electron.* **1994**, *30*, 2970.

(19) Xu, C.; Zipfel, W.; Shear, J. B.; Williams, R. M.; Webb, W. W. *Natl. Acad. Sci. U.S.A.* **1996**, *93*, 10763−10768.